Research Article

Chemical Review and Letters
journal homepage: www.chemrevlett.com
ISSN (online): 2645-4947 (print) 2676-7279

Study the efficiency of cement Kiln dust waste for removal some dyes

Farah Jabbar Ali[1], Inam Joudah Radhi[1,] *, Hamida Idan Salman[1], Saad Aziz Hassan[2]

[1]*College of Education for Pure Science, Department of Chemistry, University of Karbala, Karbala, Iraq.*
[2]*Department of chemistry, Faculty of Education for Girls Education, University of Kufa, Iraq.*

ARTICLE INFO

Article history:
Received 08 October 2024
Received in revised form 14 February 2025
Accepted 16 February 2025
Available online 16 February 2025

Keywords:
CKD,
Adsorption,
TY,
BG,
XRD,
FE-SEM,
EDX.

ABSTRACT

This study compares the adsorption behavior of Titan Yellow (TY) and Brilliant Green (BG) dyes onto cement kiln dust (CKD) powder from an experimentally simulated wastewater solution. The CKD powder was characterized using a range of techniques, including X-ray Diffraction (XRD), Field-Emission Scanning Electron Microscopy (FE-SEM), Energy Dispersive X-ray Spectroscopy (EDX), and UV-Vis absorption spectroscopy, Adsorption experiments were conducted under varying conditions, including different contact times, temperatures, pH levels, and initial concentrations of both dyes and adsorbent, using batch mode experiments. The adsorption data were analyzed using the Freundlich, Langmuir, and Temkin adsorption isotherm models. The equilibrium adsorption data were best fitted by the Langmuir and Temkin isotherms. Thermodynamic parameters, including ΔG, ΔH, and ΔS, were calculated. The results indicated that the adsorption process on CKD was exothermic and non-spontaneous for Brilliant Green, but endothermic and spontaneous for Titan Yellow. Additionally, the adsorption was highest at pH = 2 for Titan Yellow and at pH = 8 for Brilliant Green.

1. Introduction

At various phases of the dyeing and finishing processes, the textile, paper, printing, and dye industries use a lot of water . Even very little amounts of dyes can drastically alter the color of drinking water, rendering it unsafe for human consumption because these dyes are extremely poisonous, non-biodegradable, carcinogenic, and mutagenic [1].

Also, the organic or inorganic chemicals, dyes and pigments are widely employed in many industrial sectors, including carpet, paper, textile, leather, food, cosmetics, and dye manufacture. Synthetic dyes can pose serious health risks and contribute to environmental contamination because of their extensive use and large-scale production. By releasing harmful and possibly cancer-causing compounds into the environment, industrial effluent that contains leftover colored pigments into water sources causes serious pollution issues. Additionally, even trace levels of dyes result in colored effluent, which blocks sunlight and impedes photosynthesis. Consequently, industrial wastewater must be decolored before being dumped into receiving water bodies [2]. The most efficient and cost-effective method of treating wastewater containing dyes is the adsorption approach, particularly at low concentrations, the physical and chemical properties of CKD are influenced by various parameters, including the kind of kiln operation and the raw materials utilized, systems for collecting dust and the kind of fuel used to produce cement clinker. Many researchers have been working several studies on economic and efficient methods to use this dust in a number of applications such as, industrial waste water treatment, soil stabilization, cement production, agricultural fertilizers and etc [3,4]. Synthetic organic chemicals, known as dyes, come in a variety of forms, including basic, acidic, triphenylmethane, azo, sulfur, and nitro. Nitro phenol crimson (NPC) is the designation given to Titan Yellow, a derivative of 3,30,5,50 tetra nitro. The only report on the characteristics of NPV in aqueous solutions with varying acidities provides qualitative information on color transfer rather than measuring the UV-vis absorption spectra [5]. In this study, batch adsorption experiments were carried out using a UV-visible spectrophotometer see Figure 1. Brilliant green (BG) is one of the triphenyl methane based dye which has an insightful use in leather, textile and biological industries show Figure 2. Indeed, our work lies in the unique combination of cement

* Corresponding author e-mail: anaam.j@uokerbala.edu.iq
https://doi.org/10.22034/CRL.2025.479727.1443

materials and dye types, which has not been explored in previous studies.2.

1.2. Isotherms for Adsorption

Adsorption isotherm is a relationship between the equilibrium concentration of the substrate in contact with the adsorbent and the amount of adsorbate adsorbed on a specific surface at constant temperature.

1.2.1.Isotherm for Freundlich Adsorption

The following relationship exists empirically between the amount of an adsorbate absorbed per unit weight (qe(mg/g) of adsorbent and the adsorbate equilibrium concentration Ce(mg/l) in the fluid:

$$q_e = K\, C_e^{1\backslash n} \quad (1)$$

where the Freundlich coefficients are K and n. q_e = amount of adsorbent on the amount of adsorbed adsorbate, C_e = equilibrium amount of the adsorbate

$$\log(q_e) = \log K + 1\backslash n \log C_e \quad (2)$$

Log(qe) vs logCe can be plotted, and the intercept and slope can be used to get the coefficients K and n. A value of 1

1.2.2. Isotherm for Langmuir Adsorption

The adsorbent surface is thought to have several active adsorption interaction sites according to the Langmuir model. A relationship between the adsorbed substance and its equilibrium concentration was established by Langmuir [7]:

$$Ce/qe = 1/kL\ qm + Ce/qm \quad (3)$$

Where KL(L\mg) is the adsorption energy and qe (mg\g) is the amount adsorbed per unit mass of adsorbent equivalent to full coverage of sites, Ce (mg\l) is the equilibrium concentration of two dyes in solution, and qm(mg\g) is the adsorbent's monolayer adsorption capacity.

1.2.3 Temkin Isotherm

This isotherm includes a component that specifically considers the interactions between the adsorbent and the adsorbate. The model assumes that the heat of adsorption (a function of temperature) of all molecules in the layer will decrease linearly with coverage rather than logarithmically by ignoring the very low and large concentration values. Its derivation, which is represented by the equation, is characterized by a uniform distribution of binding energies (up to a maximum binding energy). The amount sorbed qe was plotted against lnCe, and the slope and intercept were used to get the constants. The following equation provides the model [8].

$$B = \frac{RT}{bT} \quad (4)$$

$$Qe = B\ln AT + B\ln C\,e \quad (5)$$

AT =Temkin isotherm equilibrium binding constant (L/g). bT = constant of Temkin isotherms. R= constant of universal gas (8.314J/mol/K). T= Temperature+-level at 298 K. B = constant connected to the sorption heat (J/mol).

The objective of this study was to extent the previous works of adsorption onto Cement Kiln Waste (CKD) for removal some dyes (Titan and Brilliant) from aqueous solutions, its studied the different temperature and different pH value and adsorption isotherms and thermodynamic parameters for two dyes.

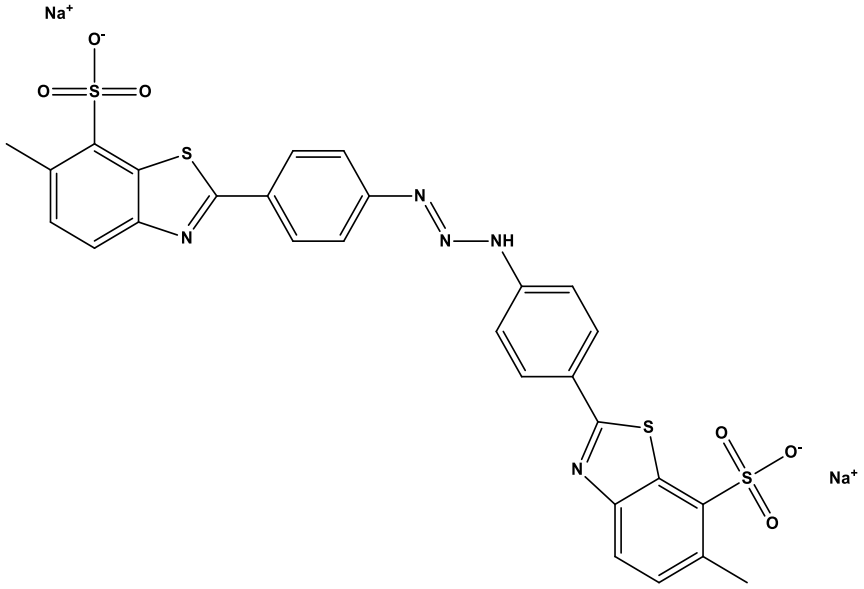

Disodium 2,2'-[(1E)-triaz-1-ene-1,3-diyldi(4,1-phenylene)]bis(6-methyl-1,3-benzothiazole-7-sulfonate)
Caution: Stereochemical terms discarded: 1e

Fig. 1. Show structure of Titan yellow dye.

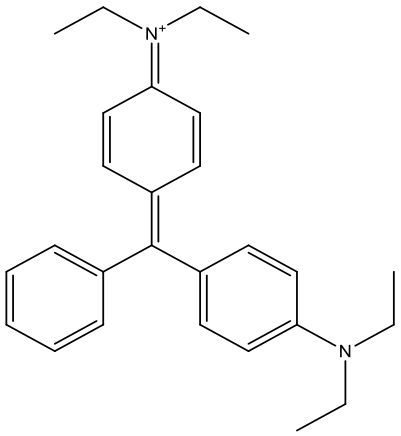

[4-[[4-(diethylamino)phenyl]-phenylmethylidene]cyclohexa-2,5-dien-1-ylidene]-diethylazanium
Computed by Lexichem TK 2.7.0 (PubChem release 2024.11.20)

Fig. 2. Show structure of Brilliant green dye.

2. Materials and methods

2.1. The features of Cement Kiln Dust (CKD)

The Portland cement facility in Al-kufa, Iraq produces a significant amount of cement kiln dust (CKD), a byproduct. It was gathered and ready for use in the adsorption experiments using the technique that has been previously mentioned. The chemical composition (wt%) of cement kiln dust is displayed in Table 1.

2.2. Preparation of CKD

To get rid of dust, CKD Waste was washed, dried, and ground. The pulverized material was then repeatedly cleaned with hot, distilled water until no color was left behind. Finally, the dried Cement Kiln Dust Waste was sieved and put away for later use.

2.3. Preparation of Titan and Brilliant dyes Solution

Titan and Brilliant dyes were added in the proper amounts to a volumetric flask containing 1000 milliliters to produce a stock solution with a concentration of 100 mg/l using distilled water. The stock solution was then diluted to the original concentrations to provide a variety of concentrations, which ranged from 10 to 50 mg/l. Figure 3, explained calibration curve was examined for all solutions at their maximum wavelengths, which were 403-406nm This is similar to a previous studies respectively [9,10], and 630 nm for Titan and Brilliant, respectively. The dyes used

in the experiment were analytical grade and came from Sigma-Alrich and BHD Chemicals Ltd. in Poole, England

2.4. The effect of contact time

In the batch adsorption procedure, 10 milliliters of Titan and Brilliant solutions at a known concentration of 50 milligrams per liter and pH of 6 were shaken in a water bath (model HH-S2, power supply: 220 V 50 Hz, China) together with the necessary amount of adsorbent (0.1 gm). The experiment was conducted at 25°C. After filtering the mixture, a spectrophotometer (EMCLAB Gmbh, model: UV-1100, Germany) every ten minutes to calculate the equilibrium time. The results showed that it took 20 minutes for Titan dye and 50 minutes for Brilliant dye, respectively, to reach equilibrium.

2.5. The effect of adsorbent dosage

To determine the optimal adsorbent dosage, experiments were carried out by adding different weights of the adsorbent, ranging from 0.2, 0.4, 0.6, and 0.8 grams, to 10 milliliters of the desired concentration of Titan and Brilliant at pH=6 and 25° C. The mixture was then agitated for 20 minutes for Titan dye and 50 minutes for Brilliant dye . To determine the concentration of Titan and Brilliant at equilibrium, a liquid concentration was assessed using a spectrophotometer. The results showed that the best weights are (0.4 g) for Titan dye and (0.8 g) for Brilliant dye respectively .

2.6. The equilibrium studies

In 50ml conical flasks containing 15ml of Titan and Brilliant solution with known starting concentrations ranging from 10 to 50 mg/l at pH=6, batch adsorption studies were conducted by adding 0.1 g of CKD. After sealing, the conical flasks were put in a shaker water bath set at 25, 35, 45, and 55 °C for 20 minutes for Titan dye and 50 minutes for Brilliant dye, respectively. Following the use of CKD adsorbent, the samples were filtered. The amount of Titan and Brilliant adsorbed, Qe (mg/g), was computed using the following equation[11] to determine the residual Titan and Brilliant concentration at equilibrium, which was quantified using spectrophotometry.

$$Qe=V(Co-Ce)/M \quad \ldots\ldots\ldots\ldots\ldots\ldots\ldots\ldots \quad (6)$$

where M is the weight of the dry adsorbent utilized in grams, Vsol. is the volume of the solution, and C_o , Ce are the initial and equilibrium Titan and Brilliant concentrations (mg/l). The following equation was used

to compute the removal efficiency[12-13]:

$$\% \text{ Removal}=((Co-Ce)/Co)*100 \quad \ldots\ldots\ldots\ldots\ldots\ldots \quad (7)$$

By adding 0.1M NaOH or diluted 0.1M HCl, the impact of pH on Titan and Brilliant adsorption was investigated in the range of (2–8).

3. Results and Discussion

3.1. Effect of adsorbent dosage

Several tests were conducted using varying adsorbent dosages at the starting Titan and Brilliant concentration of 50 mg/l. The results are displayed in Table 2 and Figure 4-15; the figure indicate that the amount of adsorption decreased as adsorbent dosage for Titan dye increased as adsorbent dosage for Brilliant dye.

3.2. Effect of contact time

To examine the effect of contact time on the percentage elimination of Titan and Brilliant from aqueous solution, experiments were carried out using an initial concentration of 50 mg/l, varied contact times from 10 to 50 minutes, pH=6, and a temperature of 25°C. The results are displayed in Figure 13 and Table 2. According to that figure, the rate of adsorption for Titan dye was rapid (20 minutes), whereas the rate of adsorption for Brilliant dye was slower at first and increased with time due to slow-passing dye ion particles in the adsorbent's internal structure.

3.3. Adsorption equilibrium

The results of testing the Freundlich, Langmuir, and Tempkin isotherms models are displayed in Figure 10-12. The Temkin and Langmuir isotherms for Titan dye were more suited for the dyes' adsorption on the surface of cement kiln dust waste. The correlation coefficient values R^2 and the notion that there was monolayer adsorption suggest that these results were consistent with previous investigations of the same surface [14] , This result correlates to the (n) value that is greater than number 1 and shows that the surface has a very high porosity and that the material distribution is either indirect or heterogeneous [15] when the Brilliant dye is applied to the tempkin isotherm; thus, demonstrates that the physical process of adsorption is advantageous for Titan dye, as determined by the Freundlich isotherm, from which the experimental constants for isotherms have been derived, as indicated in Table 3. The surface of cement kiln dust waste displays the dye isomers in the following order:

Tempkin = Langmuir > Freundlich ⟶ Titan dye

Tempkin > Freundlich > Langmuir ⟶ Brilliant dye

3.4. pH Dependence

At pH values between 2 and 8 and 25°C, the impact of pH regarding the adsorption of brilliant dyes and titanium on (CKD) was examined. The percent elimination of the dyes in relation to pH variation is displayed in Figure 6-8 and 13. This picture illustrates how the adsorption of Titan dye on the CKD surface increased as pH dropped and decreased as pH climbed show Table 4 . This is because an increase in H+ concentration causes more ions to bind with OH- ions on the CKD surface, leading to an increase in adsorption. The Table 5-7 showed that although the brilliant dye was highly adsorbent on the CKD surface at pH=8, there was also a higher likelihood of electrostatic attraction between the material and the surface. This is because the OH-ion concentration increased the amount of adsorption by adding negative charges to the surface, which increased the contradiction forces between the same ions and the surface and there was an attraction between the positively charged functional groups of dyes and the negatively charged groups on the surface. As a result, the optical disintegration of the dye increases [16].

Table 1. The chemical makeup (weight percentage) of cement kiln dust from Iraq's Al-kufa cement factory

Components	SiO_2	Al_2O_3	Fe_2O_3	CaO	MgO	SO_3	N_2	K_2O	Cl
Weight (%)	15.5	3.88	4.1	42.5	2.96	6.31	1.40	2.42	0.89

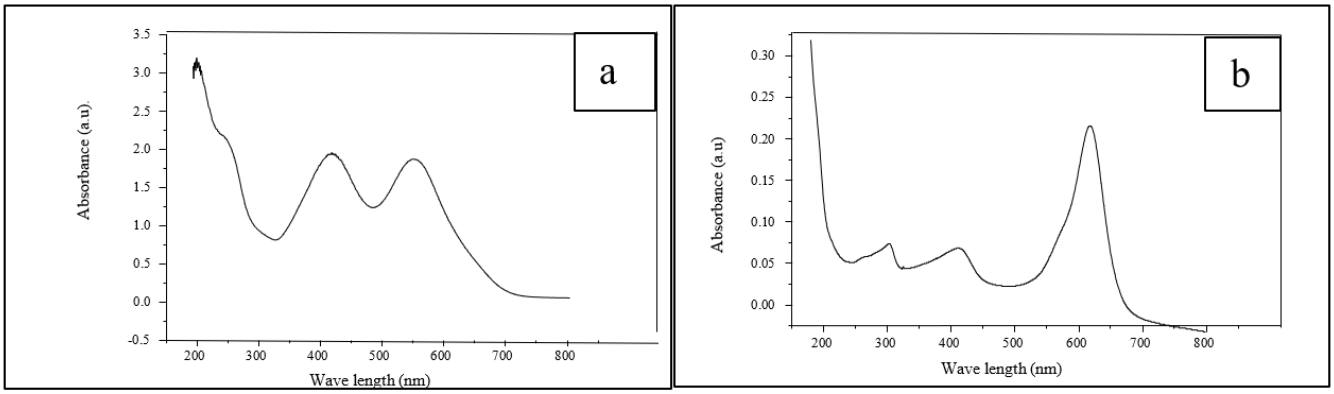

Fig. 3. (a) and (b) the The absorption spectra of Titan yellow and Brilliant Green dyes respectively.

3.5. Temperature dependence

Study has been done on the data of Titan and Brilliant adsorption on CKD at various temperatures, ranging from 25°C to 55°C. Figure 4, 6 and 14 make it evident that the removal percentage of Titan and Brilliant on CKD waste increased when the temperature was lowered. According to this, the adsorption process for Titan dye was endothermic (+ΔH), which means that adsorption rose as the temperature rose. In contrast, the process for Brilliant dye is exothermic

(-ΔH) and works best at low temperatures. [17]. To assess the thermodynamic viability of the Titan and Brilliant adsorption, which is displayed in the Table 8, thermodynamic parameters were computedThe temperature effect study can be used to assess the fundamental heat adsorption (ΔH), thermodynamic functions Gibbs energy (ΔG), and the change in entropy (ΔS) of the adsorption process.The following equation [18–19] yields the equilibrium constant (Kd) at each temperature:at every temperature [17-18] :

$$Kd=(Ce/Qe)\times(W/V)\ldots\ldots\ldots \quad (8)$$

Where :

Qe: The adsorbate's magnitude in mg/gm; Ce: The adsorbate concentration at equilibrium (mg/L); V:Volume of liquid phase; W: Weight of adsorbent

As illustrated in Figure 15, According to the Van't Hoff equation, the heat of adsorption (ΔH), calculated from plotted (ln Kd) vs (1/T), produces a straight line with slop (-ΔH/R): Ln kd = - ΔH/RT + constant adsorbate concentration (mg/L) at equilibrium

The equation is used to calculate the change in the Gibbs energy:

$$\Delta G= -RT \ln Kd \ldots\ldots\ldots\ldots \quad .(9)$$

where T is the absolute temperature in Kelvin and R is the gas constant (8.314 J K -1 mole-1). The Gibbs-Helmholtz equation is used to compute the change in entropy (ΔS)[20-21] .

$$\Delta G=\Delta H - T\Delta S \ldots\ldots\ldots\ldots \quad (10)$$

The drug's thermodynamic parameter values on cement kiln dust waste are shown in Table 8. The Gibbs free energy shift (ΔG) for Titan dye implies spontaneity, while it suggests non-spontaneity for Brilliant dye.Titan dye's ΔS° value was positive (+).implies that there was less unpredictability at the solution interface while Titan was being adsorbed, as evidenced by the Langmuir isotherm.contrast with Brilliant's adsorption on the same surface [22,23].

Table 2. Effect of adsorbent dosage and contact time on dyes adsorption.

Titan				Brilliant			
Wt. (gm)	**% R**	**Time (min.)**	**% R**	**Wt. (gm)**	**% R**	**Time (min.)**	**% R**
0.2	96	10	78	0.2	95	10	82
0.4	99.8	20	95	0.4	97	20	89
0.6	99.2	30	90	0.6	98	30	95
0.8	98	40	80	0.8	99.8	40	96
		50	75			50	99

Table 3. Values of Isotherms adsorption of dye on to CKD at different temperature and pH=6.

	289 K				308 k			318 K			328 K			
	Co (mg/L)	**ABS**	**Ce (mg/L)**	**Qe (mg/g)**	**ABS**	**Ce (mg/L)**	**Qe (mg/g)**	**ABS**	**C_e (mg/L)**	**Qe (mg/g)**	**ABS**	**C_e (mg/L)**	**Qe (mg/g)**
Brilliant	10	0.026	0.4	120	0.02	0.4	120	0.018	0.34	120.7	0.037	0.57	117.8
	20	0.029	0.49	243.8	0.032	0.5	243.7	0.042	0.7	241.2	0.05	1	237.5
	30	0.032	0.5	368.7	0.04	0.7	366.2	0.056	1	362.5	0.097	1.5	356.2
	40	0.036	0.58	492.7	0.047	0.77	490.3	0.06	1.2	485	0.153	2.5	468.7
	50	0.04	0.7	616.2	0.057	1	612.5	0.07	1.3	608.7	0.293	4	575

	289 K				308 k			318 K			328 K			
	Co (mg/L)	**ABS**	**Ce (mg/L)**	**Qe (mg/g)**	**ABS**	**Ce (mg/L)**	**Qe (mg/g)**	**ABS**	**C_e (mg/L)**	**Qe (mg/g)**	**ABS**	**C_e (mg/L)**	**Qe (mg/g)**
Titan	10	0.03	0.3	242.5	0.02	0.2	245	0.025	0.25	243.75	0.043	0.53	236.75
	20	0.043	0.53	486.75	0.023	0.23	494.25	0.057	0.77	480.75	0.05	0.7	482.5
	30	0.09	1.5	712.5	0.034	0.34	741.5	0.05	0.7	732.5	0.06	0.8	730
	40	0.15	3.5	912.5	0.089	1	975	0.04	0.5	987.5	0.08	1	975
	50	0.25	5.5	1112.5	0.19	3.9	1152.5	0.1	3	1175	0.09	1.5	1212.5

Table 4. Effect of pH on the adsorption of Titan dye on to CKD.

	pH=2				pH=4			pH=6			pH=8		
	C_o (mg/L)	ABS.	C_e (mg/L)	Q_e (mg/g)	ABS.	C_e (mg/L)	Q_e (mg/g)	ABS.	C_e (mg/L)	Q_e (mg/g)	ABS.	C_e (mg/L)	Q_e (mg/g)
Titan	**10**	**0.033**	0.3	242.5	0.031	0.3	242.5	0.03	0.3	242.5	0.027	0.2	245
	20	**0.04**	0.5	487.5	0.06	0.8	480	0.043	0.53	486.75	0.041	0.51	487.25
	30	**0.07**	0.9	727.5	0.085	1.5	712.5	0.09	1.5	712.5	0.075	0.95	726.25
	40	**0.09**	1.5	962.5	0.1	3	925	0.15	3.5	912.5	0.25	5.5	862.5
	50	**0.15**	3.5	1162.5	0.2	5	1125	0.25	5.5	1112.5	0.3	7	1075

Table 5. Effect of pH on the adsorption of Brilliant dye on to CKD.

	pH=2				pH=4			pH=6			pH=8		
	C_o (mg/L)	ABS.	C_e (mg/L)	Q_e (mg/g)	ABS.	C_e (mg/L)	Q_e (mg/g)	ABS.	C_e (mg/L)	Q_e (mg/g)	ABS.	C_e (mg/L)	Q_e (mg/g)
Brilliant	**10**	0.003	0.03	124.6	0.003	0.03	124.6	0.026	0.4	120	0.001	0.01	124.8
	20	0.006	0.06	249.2	0.005	0.05	249.3	0.029	0.49	243.8	0.007	0.07	249.1
	30	0.008	0.08	374	0.02	0.4	370	0.032	0.5	368.75	0.009	0.09	373.8
	40	0.03	0.5	493.7	0.03	0.5	493.7	0.036	0.58	492.75	0.015	0.3	496.2
	50	0.06	1.2	610	0.05	1	612.5	0.04	0.7	616.25	0.02	0.4	620

Table 6. Values of the isotherms parameters for adsorption of dyes on to CKD.

	Co(mg\l)	C_e(mg\l)	Q_e(mg\g)	C_e\ Q_e	Log C_e	Log Q_e	Ln C_e
Titan	10	0.3	242.5	0.0012	-0.522	2.384	-1.203
	20	0.53	486.75	0.001	-0.275	2.687	-0.634
	30	1.5	712.5	0.002	0.176	2.852	0.405
	40	3.5	912.5	0.003	0.544	2.960	1.252
	50	5.5	1112.5	0.004	0.740	3.046	1.704
	Co(mg\l)	**C_e(mg\l)**	**Q_e(mg\g)**	**C_e\ Q_e**	**Log C_e**	**Log Q_e**	**Ln C_e**
Brilliant	10	120	0.4	0.003	-0.39	2.079	-0.91
	20	243.8	0.49	0.002	-0.3	2.387	-0.71
	30	368.7	0.5	0.001	-0.3	2.566	-0.639
	40	492.7	0.58	0.0011	-0.236	2.692	-0.544
	50	616.2	0.7	0.0011	-0.15	2.789	-0.35

Table 7. Values of the isotherms parameters for adsorption dye on to CKD.

	Freundlich			Langmuir			Tempkin		
Titan	K_f mg-1(1-n) g-1 L1/n	n	R^2	K_L Lmg^{-1}	q_m mgm^{-1}	R^2	B $Jmol^{-1}$	A Lmg^{-1}	R^2
	15.228	2.117	0.924	0.6	1666.6	0.981	243.58	28.616	0.981
	Freundlich			**Langmuir**			**Tempkin**		
Brilliant	K_f mg-1(1-n) g-1 L1/n	n	R^2	K_L Lmg^{-1}	q_m mgm^{-1}	R^2	B $Jmol^{-1}$	A Lmg^{-1}	R^2
	27.489	0.339	0.873	-0.0005	- 175.43	0.561	935.16	2.784	0.9685

Table 8. Values of thermodynamic parameters for adsorption dye on to CKD.

	T(K)	1/T (K^{-1})	% R	pH	% R	K_d	Ln K_d	ΔH $Jmol^{-1}$	ΔG $Jmol^{-1}$	ΔS $Jmo1k^{-1}$
Titan	298	0.0033	89	2	93	5056.8	8.528	+ 36889.218	-21128.7	194.691
	308	0.0032	92.2	4	90	7387.8	8.907		-22808.2	193.822
	318	0.0031	94	6	89	9791.6	9.189		-24294.3	192.401
	328	0.003	97	8	86	20208.3	9.913		-27032.6	194.883

	T(K)	1/T (K^{-1})	% R	PH	% R	K_d	Ln K_d	ΔH $Jmol^{-1}$	ΔG $Jmol^{-1}$	ΔS $Jmo1k^{-1}$
Brilliant	298	0.0033	98.6	2	97.6	11004.4	9.306		23056.28	-236.6
	308	0.0032	98	4	98	7656.25	8.943	- 47456.312	22900.44	-228.43
	318	0.0031	97.4	6	98.6	5853.3	8.674		22932.77	-221.34
	328	0.003	92	8	99.2	1796.8	7.493		20433.35	-206.98

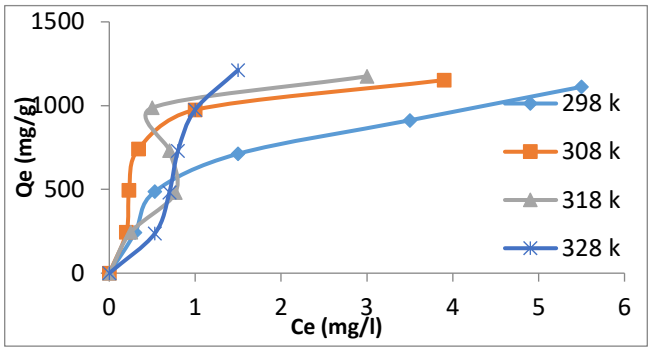

Fig. 4. Isotherms of adsorption of Titan dye on the CKD at different temp

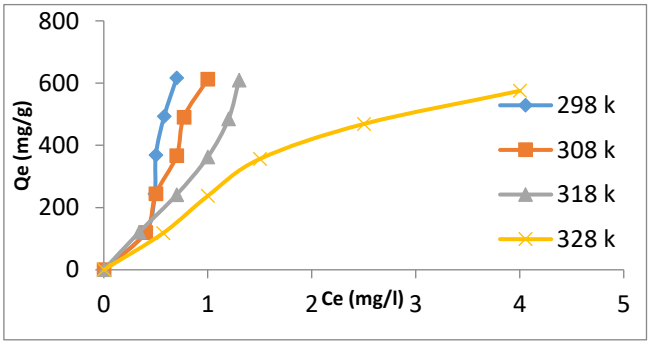

Fig. 5. Isotherms of adsorption of Brilliant dey on the CKD at different temp

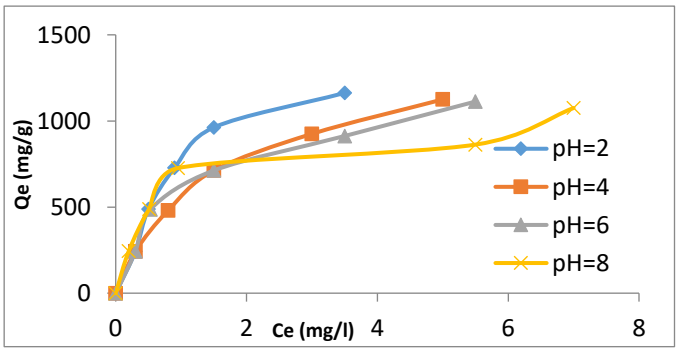

Fig. 6. Isotherms of adsorption of Titan dye on the CKD at different pH

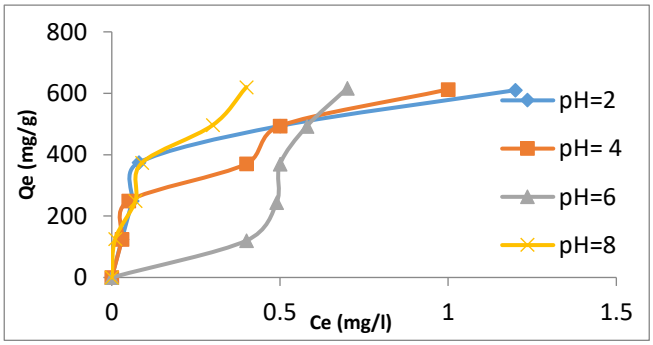

Fig. 7. Isotherms of adsorption of Brilliant dye on the CKD at different pH

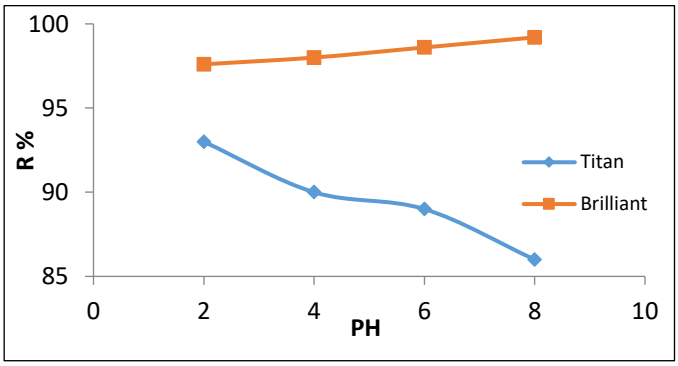

Fig. 8. Effect of pH on the percent removal of Titan and Brilliant dyes on the CKD

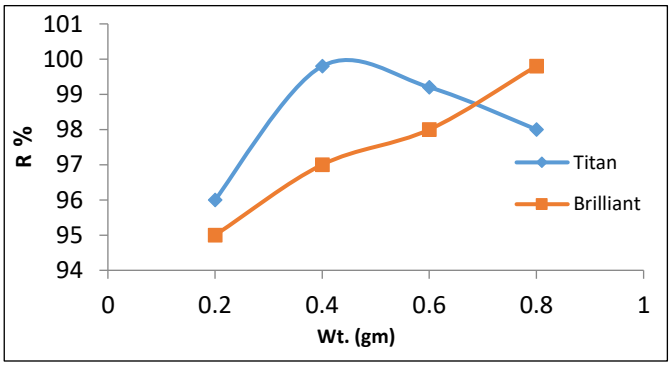

Fig. 9. Effect of whieght on the percent removal of Titan and Brilliant deys on the CKD at pH=6, temperature 25°C

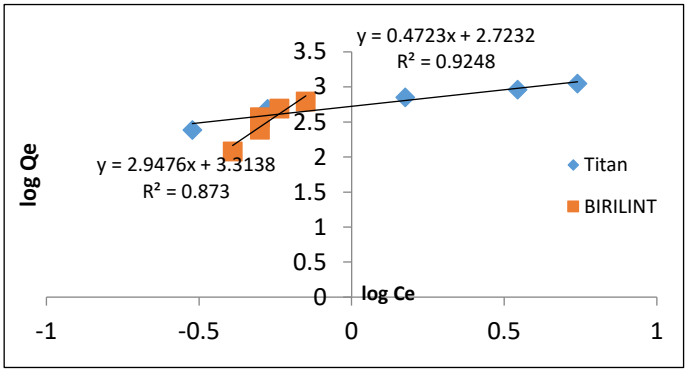

Fig. 10. Freundlich equation for the adsorption of Titan and Brilliant deys on the CKD

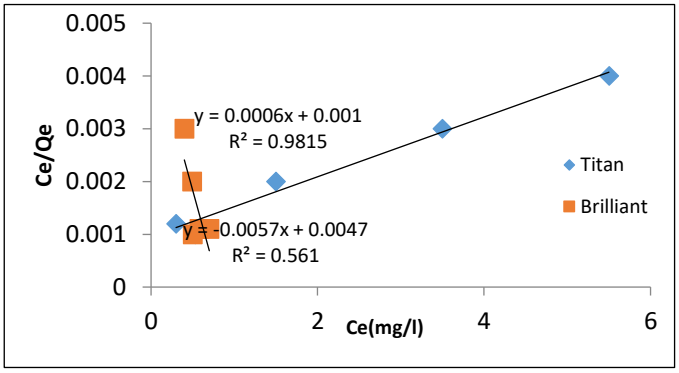

Fig. 11. Langmauir equation for the adsorption of Titan and Brilliant deys on the CKD

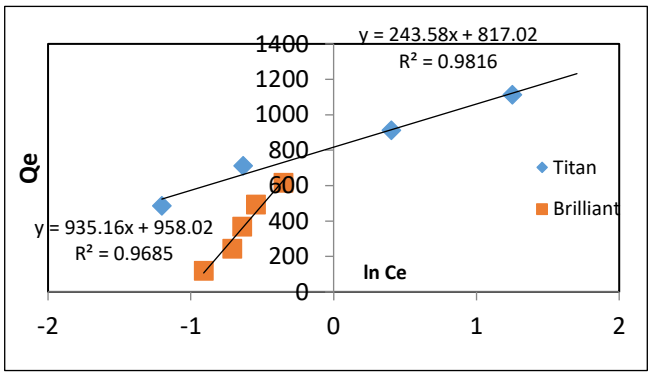

Fig. 12. Temkin equation for the adsorption of Titan and Brilliant deys on the CKD

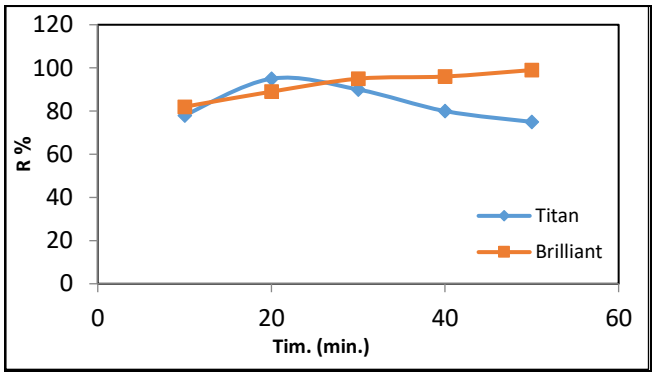

Fig. 13. Effect of contact time on the percent removal Titanand Brilliant deys on the CKD at pH=6, temperature 25°C

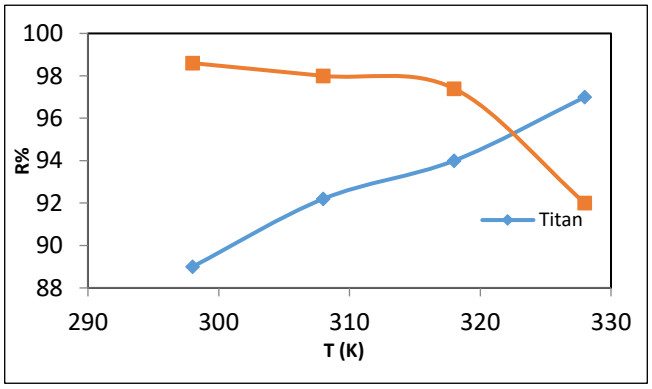

Fig. 14. Effect of temperature on the percent removal of Titan and Brilliant deys on the CKD

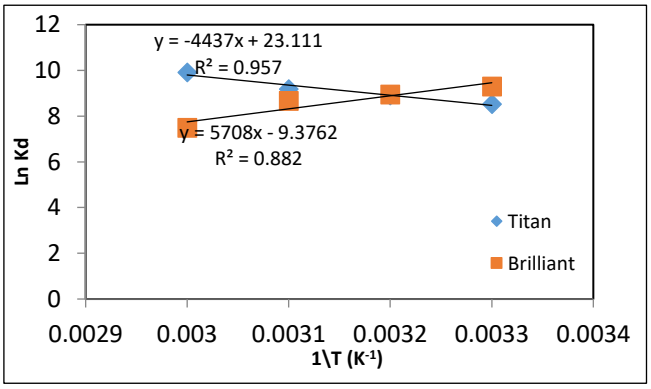

Fig. 15. Relationship between temperature and Ln K_d of Titan and Brilliant deys on the CKD at pH=6, temperature 25°C

3.6. Characterization of the starting CKD

X-ray diffraction (XRD) is a widely used method for figuring out a material's mineralogical composition [24]. Figure 16 displays the minerals found in the examined samples by XRD analysis, demonstrates that, in addition to portandite (Ca(OH)2), the primary constituent phases of CKD were calcite ($CaCO_3$) 26.806, 29.683, 36.241, 43.463.47.596, and 48.701, quartz (SiO_2) 23.371, 24.804, 57.601, 60.896, and 64.347, and lime (CaO) 1. 187, 42. 453, 84. 034, and 95. 224. It is likely that MgCO3, Fe3O4, and Al_2O_3 will existHowever, because its distinctive reflections are so similar to those of $CaCO_3$, it is difficult to tell them apart. The amount of CaO that is easily accessible for reactions is indicated by the presence of lime. Because of the aforementioned components, which are essential for the precipitation of heavy metals, CKD tends to exhibit increased alkalinity behavior [25].

The best analytical method for describing and displaying a specimen's elemental composition is field emission scanning electron microscopy (FE-SEM). [26].

Particles of a variety of shapes, ranging from 10 to 50 µm, were seen in the FE-SEM micrographs of the samples under study. To make a differentiation, the FE-SEM pictures were taken at different magnification ranges both before and after the adsorption procedure [27].

FE-SEM can create a real, crisp image, it can be used to characterize the adsorbents and determine their structural makeup. These pictures demonstrate how CKD particles have an uneven surface, varying in size and shape, and having numerous pores that might hold the adsorbate. With their finely packed, clustered crystals that tend to clump together more, they roughly resemble a "popcorn structure." [28].

EDX stands for energy-dispersive X-ray spectroscopy. Right here. As seen in Figure 17 (a-b). EDX analysis concurrently identified Si, Al, Mg, Fe, and Na as metallic elements and (O,C) as non-metallic elements. Because of its excellent cementitious qualities, ground granulated blast-furnace slag (GGBFS) is utilized in the Fe. The EDX data's primary elements (Ca, Na, Si, Al, Mg, and O) suggest that the slag analyzed is blast furnace slag [29]. Ferrite phases are indicated by the elongated or prismatic particles, while aluminate phases are characterized by fine to lath-like crystals made up of a matrix between ferrite crystals[30-32]. Dolomite and the three primary calcium carbonate polymorphs—vaterite, aragonite, and calcite—were discovered to be present in various samples by the study. In the limestone sample, calcite is the most stable form of calcium carbonate and the ruling mineral (Figure 18 (a-b)) [32,33].

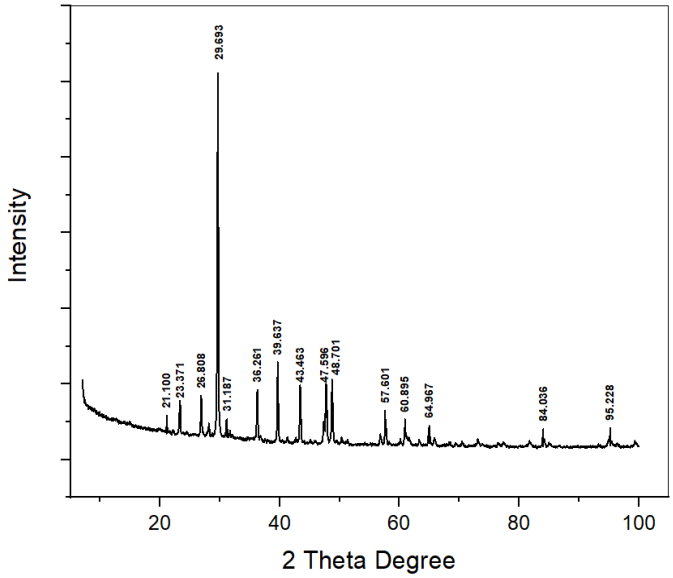

Fig. 16. X-ray diffraction spectrum of CKD.

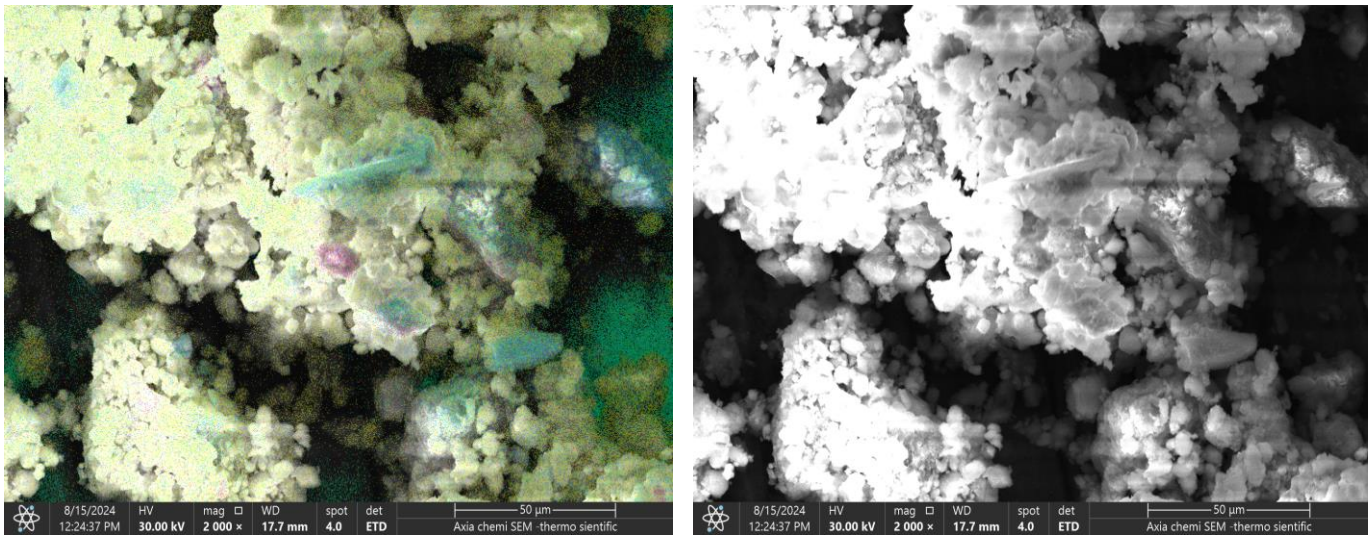

(a) (b)

Fig. 17. Real image FE-SEM illustrations of pure cement kiln dust (CKD) (a–b).

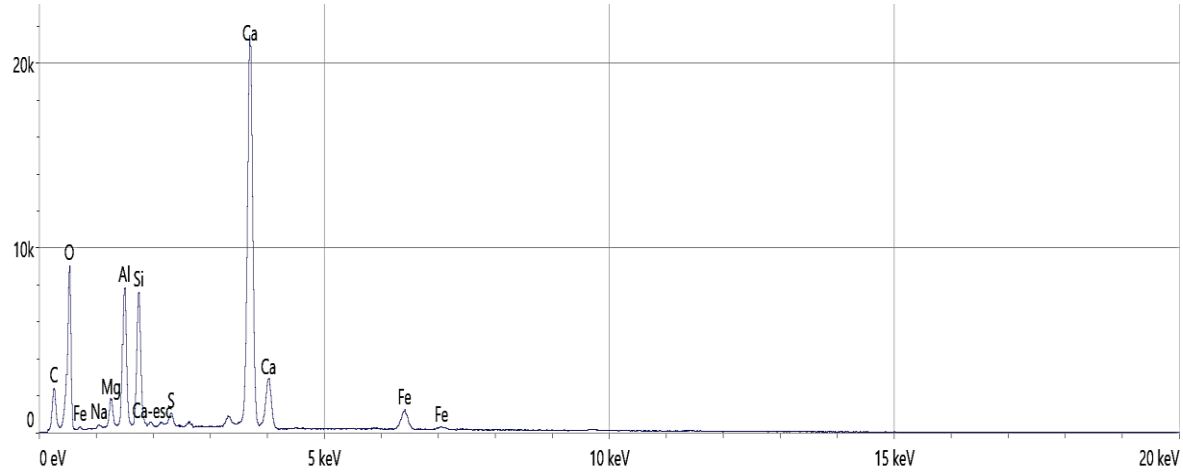

Fig. 18. (a)

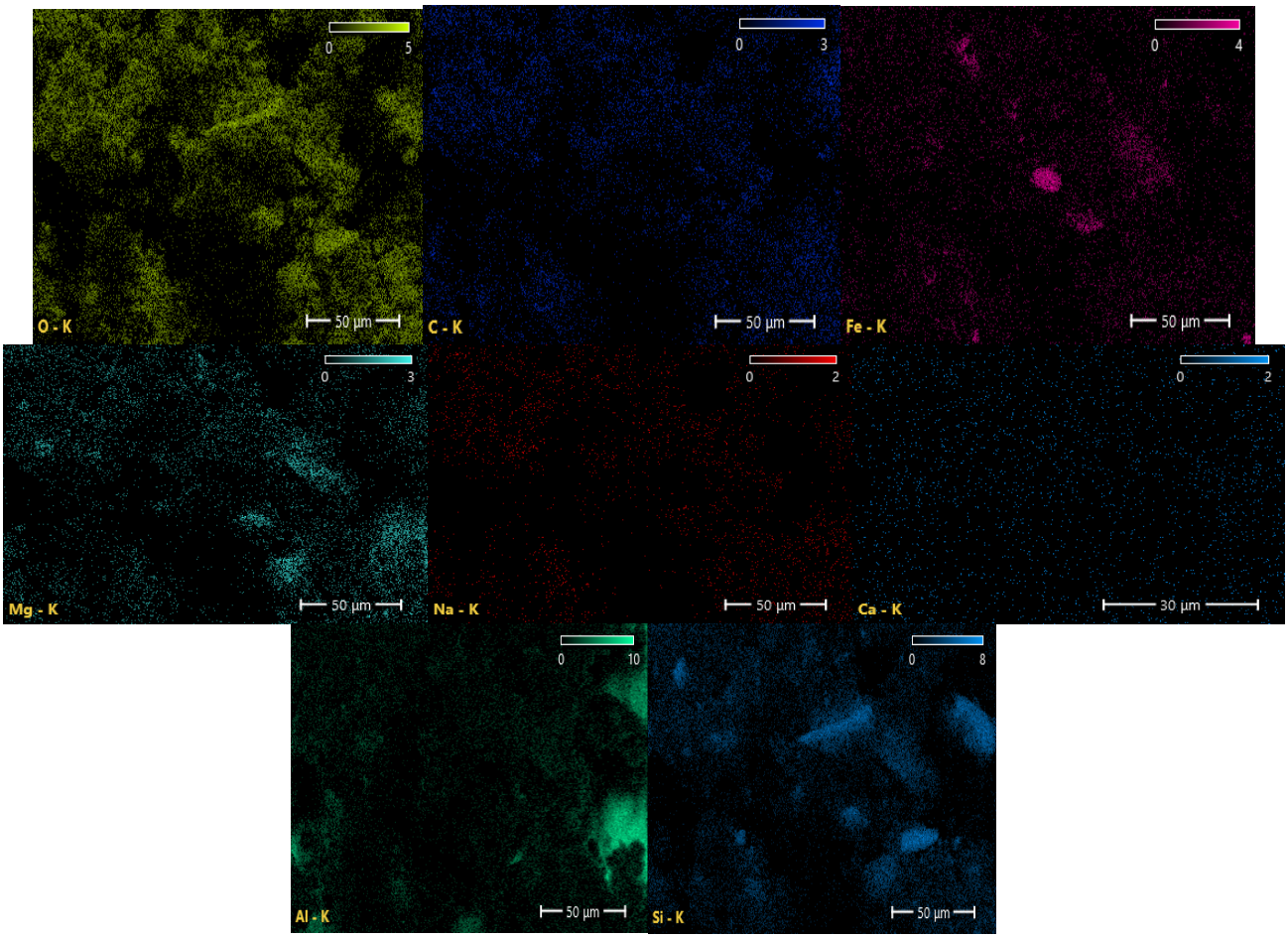

Fig. 18. (b)

Fig. 18. Real image of EDX analysis of CKD (a-b).

4. Conclusion

In the current work, we synthesized an inexpensive and readily available adsorbent from an aqueous solution for the batch system-based adsorption of Titan and Brilliant dyes on CKD. The CKD powder 'the adsorbent in this study' was characterized by using the XRD, FE-SEM,EDX tests and theoretical studies. The results showed that in an equilibrium response, the adsorption efficacy sharply decreased as temperature and particle size increased. The Langmiure and Temkin isotherm model provided a better fit for the adsorption process when compared to other relevant isotherm models. The thermodynamic analysis of adsorption produced values for Gibbs free energy (ΔG°) and enthalpy (ΔH°), demonstrating that the adsorption process on CKD was exothermic and non-spontaneous in Brilliant dye, but endothermic and spontaneous in Titan Yellow. It was also

observed that adsorption was regular and nonrandom in pH (2–8), titan dye had a height at pH=2, but brilliant dye had a height at pH= 8. Date pits are a very successful adsorbent for eliminating colors from aquatic environments, according to the study's. Finally, this article pointed out the utilization of one of the industrial hazardous pollutants, i.e., CKD, in the treatment of simulated polluted wastewater, realizing that CKD powder can be a practical adsorbent with little cost for the effective removal of dyes from industrial wastewater achieving an environmental and economical solution for the addressed issues simultaneously at the same time.

References

[1] H. Abdulmumini, A. M. Ayuba, Raw water lily leaves (Nymphaea lotus) powder as an effective adsorbent for the adsorption of malachite green dye from aqueous solution, *Chem. Rev. Lett.*, 5 (2022) 250-260.

[2] M. Rohani Moghadam, S. Pirozi, F. Beigmoradi, A. Bazmandegan-Shamili, H. Masoodi, Application of response surface methodology for modeling and optimization of basic yellow 28 decolorization using sonoelectrochemistry, *Chem. Rev. Lett.*, 6 (2023) 15-23.

[3] H. Salman, H. I. Idan, M. J. Manshad, Inhibitive action of Cresol red dye on the corrosion of mild steel alloy in 1M H2SO4, *AIP Conf. Proc.*, 2414 (2023) 1-7.

[4] A. M. Ayuba, M. Sania, Alizarin Red S dye removal from synthetic effluent solution using untreated Typha grass adsorbent, *Chem. Rev. Lett.*, 6 (2023) 340-349.

[5] H. Shafiekhani, F. Mostaghni, N. M. Mahani, Design selective Cu^{2+} chemo-sensor based on Bis-Azo dye for determination of Cu^{2+} in water samples, *Chem. Rev. Lett.*, 7 (2024) 404-412.

[6] B. Meroufel, O. Benali, M. Benyahia, Y. Benmoussa, M. A. Zenasni, Adsorptive removal of anionic dye from aqueous solutions by Algerian kaolin: Characteristics, isotherm, kinetic and thermodynamic studies, *J. Mater. Environ. Sci.*, 4 (2013) 482-491.

[7] D. O. Omokpariola, Experimental modeling studies on the removal of crystal violet, methylene blue, and malachite green dyes using Theobroma cacao (Cocoa Pod Powder), *J. Chem. Lett.*, 2 (2021) 9-24.

[8] S. Hadadian, L. Dolatyari, B. Farajmand, M. R. Yaftian, Methylene blue elimination from contaminated water solutions using a polyvinyl chloride based polymer inclusion membrane containing bis(2-ethylhexyl) phosphoric acid, *Chem. Rev. Lett.*, 7 (2024) 311-324.

[9] P. O. Ameh, Utilization of nanoparticle prepared from local Nigerian hen egg shell as an adsorbent for the removal of methylene blue dye from aqueous solution: DFT and experimental study, *Chem. Rev. Lett.*, 5 (2022) 29-43.

[10] S. Arabi, Adsorption of Orange 3R by chitosan modified montmorillonite nanocomposite, *Chem. Rev. Lett.*, 6 (2022) 55-65.

[11] P. O. Ameh, Utilization of nanoparticle prepared from local Nigerian hen egg shell as an adsorbent for the removal of methylene blue dye from aqueous solution: DFT and experimental study, *Chem. Rev. Lett.*, 5 (2022) 29-43.

[12] S. Arabi, Adsorption of Orange 3R by chitosan modified montmorillonite nanocomposite, *Chem. Rev. Lett.*, 6 (2023) 55-65.

[13] F. M. Hussein, H. I. Salman, A. A. Balakit, Adsorption isotherm of methyl orange on cross-linked chitosan Schiff base/TiO_2 nanocomposite, *AIP Conf. Proc.*, 2414 (2023) 1-7.

[14] S. Khammarnia, J. Saffari, M. S. Ekrami-Kakhki, Synthesis of $La_2MnFe_2O_7$ and $La_2CuFe_2O_7$ magnetic nanocomposites (nano mixed metal oxides) as efficient photocatalyst for organic dye removal, *Chem. Rev. Lett.*, 7 (2024) 123-133.

[15] A. Akrami, A. Niazi, Synthesis of maghemite nanoparticles and its application for removal of Titan yellow from aqueous solutions using full factorial design, *Desalination Water Treat.*, (2016) 1–14, doi:10.1080/19443994.2015.1136693.

[16] S. Khammarnia, J. Saffari, M. S. Ekrami-Kakhki, Synthesis of $La_2MnFe_2O_7$ and $La_2CuFe_2O_7$ magnetic nanocomposites (nano mixed metal oxides) as efficient photocatalyst for organic dye removal, *Chem. Rev. Lett.*, 7 (2024) 123-133.

[17] S. A. Hassan, F. J. Ali, Assessment of the Ofloxacin (Novecin) adsorption from aqueous solutions by two agricultural wastes, *Int. J. Adv. Sci. Tech. Res.*, 2 (2014) 4.

[18] F. Loulidia, B. Boukhlifia, M. Ouchabib, A. Amara, M. Jabria, A. Kalia, F. Aziz, Kinetic, isotherm and mechanism investigations of the removal of Basic Violet 3 from water by raw spent coffee grounds, *Phys. Chem. Res.*, 8 (2020) 3, DOI: 10.22036/pcr.2020.225170.1751.

[19] S. A. Hassan, F. Jabbar Ali, Equilibrium, thermodynamics and kinetics study of doxycycline adsorption from aqueous solution using spent black tea leaves and pomegranate peel wastes, *Int. J. Dev. Res.*, 4 (2014) 1, pp. 129-135.

[20] A. K. Ibrahim, S. H. Ahmed, R. A. Abduljabbar, Adsorption of Congo Red dye from aqueous solutions using an eco-friendly adsorbent derived from buckthorn fruits, *Tikrit J. Eng. Sci.*, 31 (2024) 1, 182-192, doi.org/10.25130/tjes.31.1.16.

[21] F. Jabbar Ali, H. K. A., N. T. T., N. H., H. H. T., Adsorption of metronidazole benzoate from aqueous solution by using pomegranate peel: A thermodynamics study, *Drug Invention Today*, 11 (2019) 1-6.

[22] P. O. Ameh, Removal of methylene blue from aqueous solution using nano metal oxide prepared from local Nigerian hen egg shell: DFT and experimental study, *Chem. Rev. Lett.*, 6 (2022) 29-43.

[23] F. Eltaboni, A. Al Balazi, M. S. Al Warfaly, Thymol blue release from dried polyacrylamide filmogenic solution coated on a quartz cell: One-shot study, *J. Chem. Lett.*, (2024).

[24] P. Praveendaniel, R. A. Selvan, Synthesis and application of TiO_2-phosphomolybdic acid nanocomposite, *J. Chem. Lett.*, 4 (2023) 117-129.

[25] H. M. Al Tameemi, et al., Expulsion of cadmium from a simulated wastewater using CKD as adsorbent: Optimization with isotherm study, *Periodicals of Engineering and Natural Sciences (PEN)*, 9 (2021) 998-1015.

[26] I. J. Radhi, S. A. Hassan, A. F. Alkaim, Preparation and characterization of ZnO, WO_3/ZnO nanocomposites using hydrothermal method, *J. Nanostructures*, (2023).

[27] E. Syala, W. A. Sadik, A. G. M. El-Demerdash, W. Mekhamer, M. E. El-Rafey, The effective treatment of dye-containing simulated wastewater by using cement kiln dust as an industrial waste adsorbent, *Scientific Reports*, 14 (2024) 14589.
[28] R. Oduola, Chemical and mineralogical analyses of cement-kiln-dust (CKD) and its potential impact on the environment, *3rd International Conference on Atmospheric Dust*, (2018).
[29] Z. B. Alam, K. A. B. M. Mohiuddin, Micro-characterization of dust and materials of dust origin at a cement industry located in Bangladesh, *Aerosol Air Qual. Res.*, 23 (2023) 220109.
[30] B. Suryadevara, ed., Advances in chemical mechanical planarization (CMP), Woodhead Publishing, (2016).
[31] S. P. Thomas, A. Singh, A. Grosjean, K. Alhameedi, T. B. Grønbech, R. Piltz, A. J. Edwards, B. B. Iversen, The ambiguous origin of thermochromism in molecular crystals of dichalcogenides: Chalcogen bonds versus dynamic Se−Se/Te−Te bonds, *Angew. Chem. Int. Ed.*, 62 (2023) e202311044.
[32] A. Singh, A. K. Avinash, L. A. Malaspina, M. Banoo, K. Alhameedi, D. Jayatilaka, S. Grabowsky, S. P. Thomas, Dynamic covalent bonds in the ebselen class of antioxidants probed by X-ray quantum crystallography, *Chem. – Eur. J.*, 30 (2024) e202303384.
[33] I. Manisalidis, et al., Environmental and health impacts of air pollution: A review, *Front. Public Health*, 8 (2020) 14.
[34] D. Y. TE, K. Alhameedi, J. J. Fifen, M. Nsangou, Structures, binding and clustering energies of $Cu^{2+}(MeOH)_n$ (n=1-8) clusters and temperature effects: A DFT study, *Polyhedron*, 234 (2023) 116343.